HOSTED BY

ELSEVIER

Available online at www.sciencedirect.com

ScienceDirect

Soils and Foundations 60 (2020) 840–855

www.elsevier.com/locate/sandf

Technical Paper

Freeze-thaw durability and shear responses of cemented slope soil treated by microbial induced carbonate precipitation

Sivakumar Gowthaman [a,*], Kazunori Nakashima [b], Satoru Kawasaki [c]

[a] *Division of Sustainable Resources Engineering, Graduate School of Engineering, Hokkaido University, Kita 13, Nishi 8, Kita-Ku, Sapporo, Hokkaido 060-8628, Japan*

[b] *Division of Sustainable Resources Engineering, Faculty of Engineering, Hokkaido University, Kita 13, Nishi 8, Kita-Ku, Sapporo, Hokkaido 060-8628, Japan*

[c] *Division of Sustainable Resources Engineering, Faculty of Engineering, Hokkaido University, Kita 13, Nishi 8, Kita-Ku, Sapporo, Hokkaido 060-8628, Japan*

Received 19 September 2019; received in revised form 31 March 2020; accepted 24 May 2020
Available online 11 August 2020

Abstract

Instability of slope soils under varying nature is one of the serious concerns in geotechnical engineering. Microbial induced carbonate precipitation (MICP) is a recently emerged, biological ground improvement technique, and that has the potential to enhance the shear strength, modify the surface conditions and promote the stability of deposits. This paper presents the experimental works conducted to investigate the durability and shear responses of MICP treated slope soil, demonstrating the feasibility of technique as potential alternative for slope soil stabilization. The first objective is to investigate the freeze–thaw (FT) response of MICP specimens, because FT cycles can affect the aggregate stability in regions with seasonal frost, which in turn impacts runoff and erosion in slopes. FT tests were performed as a credible indicator of durability, and the subjected specimens were monitored nondestructively (mass loss, S-wave, P-wave velocities). Secondly, shear tests were performed, and effective strength properties were analyzed at peak and residual states. FT test results suggest that contact cementation provides additional resistive forces in slope soil against progressive expansion of pore water during FT; however, aggregate stability is attributed to adequate cementation level which facilitates effective particle contacts. Shear test results indicate that MICP has influence on friction and cohesion parameters. However, the residual strength is mainly contributed by friction angle, only a minor effect from cohesion.

Keywords: Slope soil; Cementation level; Durability; Freeze–thaw response; Shear response

1. Introduction

The improved engineering response of cemented soils contributed to the developments of artificial cementation methods for soil stabilizations. Over many decades, numerous cementation-based soil stabilization methods have been developed, and those are widely applied in geotechnical projects globally (DeJong et al., 2006). Microbial induced carbonate precipitation (MICP) is one of the cementation-based soil stabilization techniques, very recently emerged and has drawn a great deal of interest among geotechnical engineers worldwide. The technique relies on set of biological and biochemical reactions, utilizing bacterial enzyme to produce calcium carbonate biocement in the in situ soil matrix, leading improvements in engineering properties of soil (Montoya and De Jong,

Peer review under responsibility of The Japanese Geotechnical Society.

* Corresponding author at: Graduate School of Engineering, Hokkaido University, Kita 13, Nishi 8, Kita-Ku, Sapporo, Hokkaido 060-8628, Japan.

E-mail addresses: gowtham1012@outlook.com (S. Gowthaman), nakashima@geo-er.eng.hokudai.ac.jp (K. Nakashima), kawasaki@geo-er.eng.hokudai.ac.jp (S. Kawasaki).

https://doi.org/10.1016/j.sandf.2020.05.012

2015; van Paassen et al., 2010; Whiffin et al., 2007). The soil bacteria which have the urease producing potential (have also been defined as ureolytic bacteria), play a very important role, which induces the urea hydrolyzes to produce ammonium and carbonate ions in the aqueous medium. In the presence of calcium ions in reaction media, the calcium carbonate bio-cement precipitates (Bao et al., 2017; Mujah et al., 2017; Ng et al., 2012; Soon et al., 2014). The reactions occurred during the process are presented as follows:

$$H_2N - CO - NH_2 + 2H_2O \xrightarrow{\text{urease}} CO_3^{2-} + 2NH_4^+ \quad (1)$$

$$Ca^{2+} + CO_3^{2-} \rightarrow CaCO_3(\downarrow) \quad (2)$$

The precipitated calcium carbonate would cement the soil particles at the contact points, coat the soil particles and partially fill the voids with or without bridging the soil particles, improving the mechanical and geotechnical properties of soil (DeJong et al., 2010; Feng and Montoya, 2016; Lin et al., 2016; Montoya and De Jong, 2015). Researchers have reported that the MICP treatment could increase the shear strength and stiffness of the soil (Feng and Montoya, 2016; Lin et al., 2016; Montoya and De Jong, 2015), while reducing the settlement (van Paassen et al., 2010). Within a couple of decades, many studies have demonstrated the feasibility of the MICP technique for various geotechnical applications including soil improvement (Amarakoon and Kawasaki, 2018; Cheng and Cord-Ruwisch, 2014; Martinez et al., 2013), liquefaction control (Montoya et al., 2013), erosion control (Jiang and Soga, 2017), fugitive dust control (Meyer et al., 2011), and coastal protection (Danjo and Kawasaki, 2016), advancing the MICP towards field implementation. Despite of the substantial interest on this technique, available information on the durability responses of MICP treated soils are still very limited, and a deeper understanding is essential prior to the in-situ implementations.

Erosion is one of the most common slope degradation process, and which is primarily persuaded by rainfall and snow melt (Fox et al., 1997; Rieke-Zapp and Nearing, 2005). Up to now, only few studies have investigated the erodibility of MICP treated deposits through various strategies. Salifu et al. (2016) have investigated the erodibility response of the MICP treated small foreshore slopes under tidal wave effects and suggested the significant increase in stability of treated surface. By using the simple fume tests, Bao et al. (2017) have demonstrated the surface stability of MICP treated cohesionless sand against scouring. Potential of MICP in controlling seepage-induced internal erosion of gravel-sand mixtures has also been examined by few researchers, suggested that the formation of calcite clusters is responsible for reduction in erosion (Jiang and Soga, 2019, 2017). Very recently, surface erosion of sandy slope was studied under simulated rainfall (5 mm/min), showed that erosion resistance was higher in slopes treated using 0.2–1 mol/L compared to that treated using 2 mol/L (Jiang et al., 2019). It is worth noting that there are, however, no studies found regarding the deployment of MICP to control the erosion induced by cyclic freeze–thaw effects.

The research work addressed herein focus on investigating the feasibility of MICP technique as an alternative remedial measure for slope soil stabilization. The flow-chart (Fig. 1) presents the sequence of the entire works that have already been performed (Steps 1–4), together with the future tasks to be performed in subsequent steps (Steps 5–6). In our previous works (Gowthaman et al., 2019a,b) (indicated by Steps 1 and 2), the potential ureolytic bacteria were identified from the target slope, and their growth and enzymatic performances were extensively studied and optimized under various physical and chemical conditions. Considering the effect of grain size distribution, the feasibility of bio-augmentation on stabilizing slope soils has also been well demonstrated using column specimens. As shown in Fig. 1, this paper presents the experimental works conducted to investigate the durability and shear responses of MICP treated slope soil which is representative of erosion prone expressway slope in Onuma (Hokkaido, Japan). Soils in cold regions usually experience frosting during winter seasons, resulting profound effects on stability and erodibility of soil along the slopes (Ferrick and Gatto, 2005; Gatto, 2000). The erosions were also documented to be the highest during snow melting, and the surface runoff had significant potential to detach the particles from thawed soil surface (Kværnø and Øygarden, 2006). It is clear that freeze–thaw durability analysis is crucial for MICP treated deposits exposing seasonal frosts, and those responses have not been extensively investigated up to now. Therefore, one of the objectives of this study was to find out whether the MICP treated slope soil was affected by cycles of freezing and thawing and to quantify the effects.

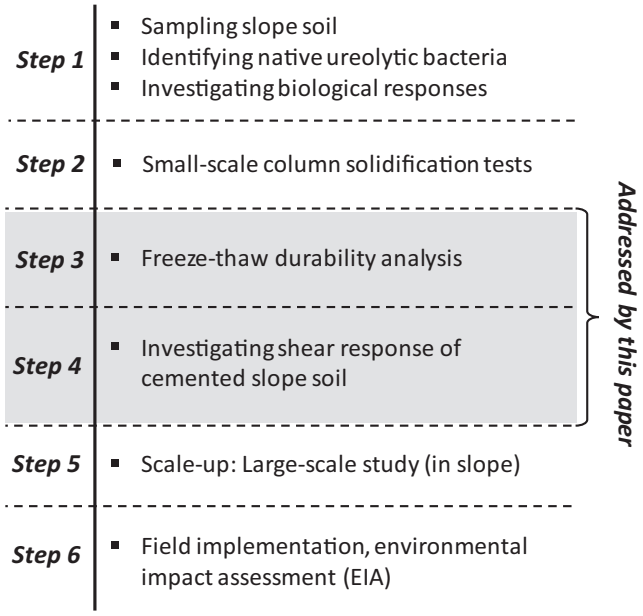

Fig. 1. Complete flow-chart of research works (slope soil stabilization).

In order to make a deeper understanding on the mechanical behavior, shear responses of MICP treated slope soil in both peak and residual states were investigated as the second objective of this study. In the above both objectives, slope soils treated to different treatment levels ranging 12–23% ($CaCO_3$ by weight) were investigated, and the results are discussed in detail.

2. Materials and experimental procedures

2.1. Residual soil

Residual soil collected from the target slope (Onuma, Hokkaido, Japan) was used in the experiments. Fig. 2a and 2b present the particle size distribution and physical appearance of the slope soil, respectively. The soil mostly consists of fine sand has the particle diameter at 50% finer by mass (D_{50}) of 0.23 mm, coefficient of uniformity (C_u) of 2.5 and coefficient of curvature (C_c) of 0.8. Results of chemical analysis performed using Energy Dispersive X-Ray Fluorescence (XRF) spectrometer (JSX-3100R II JOEL, Japan) reveal that the slope soil majorly consists of SiO_2, Al_2O_3, Fe_2O_3, CaO, MgO and K_2O of 57.5%, 25.6%, 8.1%, 3.68%, 1.99% and 1.05%, respectively. The average moisture content and pH of the natural soil were 10.5% and 6.99, respectively. Considering the field application, soil was directly used for the MICP study at its natural conditions without any pretreatments.

2.2. Bacteria and cementation media recipe

Lysinibacillus xylanilyticus, the gram-positive ureolytic bacteria, identified and isolated from the native slope soil were used in this research study. The procedure of isolation and biological characterization of the bacteria can be found in Gowthaman et al. (2019b). Bacteria were cultivated in ATCC specified NH_4-YE medium (Table 1) at 25 °C and 160 rpm under sterile aerobic conditions. After 48 h of shaking incubation, bacteria were harvested at the optical density value (measured at a wavelength of 600 nm) ranging between 4 and 4.5, and the urease activity was around 3 U/mL. Table 1 presents the chemical recipes of bacteria and cementation media that were used in this study.

Table 1
Chemical recipe of mediums.

Medium	Constituents
Bacteria growth medium (100 mL)	1.57 g of tris buffer 2 g of yeast extract 1 g of ammonium sulfate
Cementation solution (100 mL)	11.1 g of calcium chloride 6 g of urea 0.6 g of nutrient broth

2.3. Specimen preparation and MICP treatment

The soil was packed in vertically positioned syringe columns (30 mm in diameter; 50 mm in height) to a density of 1.6 ± 0.1 g/cm^3 (the corresponding relative density was around 60%). The treatment temperature was the same as the bacteria cultivation temperature (25 °C). A two phase injection strategy was used to treat the soil, similar to that reported in many previous studies (Cheng and Cord-Ruwisch, 2014; Feng and Montoya, 2016; Lin et al., 2016). In the first phase, the bacteria culture prepared in accordance with the proportions provided in Table 1 was introduced to the top column. After 2 h, 10 mL of the cementation solution (Table 1) was injected similar to that of biological injection. All the solutions introduced to the top column were allowed to percolate and drain out under gravitational and capillary forces. The cementation solution was injected every 24 h during the treatment. The injection interval of 24 h was chosen on the basis of effective crystallization, despite of the impacts on construction schedules and cost. The size of produced MICP crystals are highly dependent on the time interval between cementation solution injections, determining the stability and strength of MICP soils. For instance, the average size of $CaCO_3$ crystals was found to be considerably high when the injection interval was 23–25 h compared to the lower injection intervals (Wang et al., 2019).

Typically, the activity of the soil bacteria starts to decrease after 6–8 injections of cementation solution, and

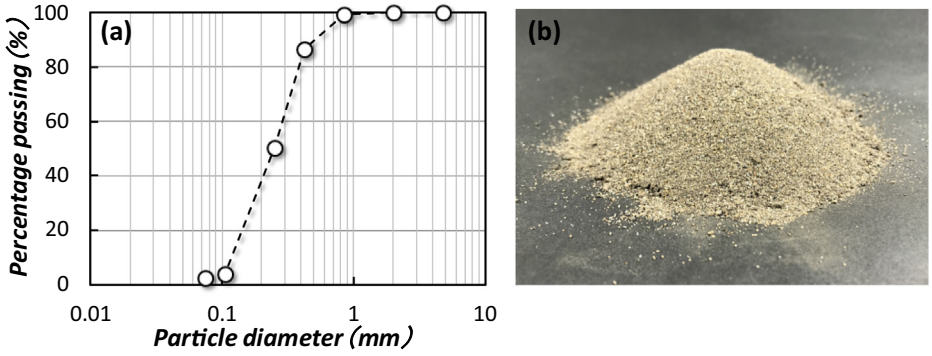

Fig. 2. Slope soil (Onuma, Hokkaido, Japan) (a) gradation curve and (b) physical appearance.

this was herein observed by the drop in pH and increase in Ca^{2+} ion concentration at the effluent. Therefore, the biological injection was performed once again on seventh day (after 7 injections of cementation media) to maintain the bacterial activity.

Different durations of treatment were undertaken to obtain different levels of cementation. In this paper, three levels of cementation were considered: Level 1, Level 2 and Level 3. For Level 1 cementation, 7 injections of cementation solution were applied. Total number of 10 and 14 cementation injections were performed for Level 2 and Level 3, respectively. Concentration of Ca^{2+} ions and pH were measured at the outlet during the treatment, and the measurements indicated the high chemical conversion efficiency (above 80%), suggesting the effective utilization of resources in slope soil studied herein. The average calcium carbonate content of 12–14% by mass is considered as Level 1 cementation, and Level 2 and Level 3 cementations are defined as 16–18% and 21–23%, respectively. In fact, these levels fall under the "heavy cementation" category defined systematically (based on the soil state, geologic age and behavior) by previous researchers (Feng and Montoya, 2016; Montoya and De Jong, 2015). The average calcium carbonate content was determined using the method described in the subsequent section.

After the completion of MICP treatment, specimens were rinsed by using tap water of five times of pore volume in order to remove all the existing salts and chemicals. It was suspected that the existence of unreacted chemicals might yield additional products, leading to the variations in experimental responses than the actual ones. However, the rinsing is not mandatory during field applications, as the presence chemicals does not adversely affect. All the specimens that were removed carefully from the syringe columns, were carefully trimmed to a height of 30 mm prior to the experimentations.

2.4. Measurement of $CaCO_3$ content

Carbonate content was determined by a simplified device developed to measure the pressure of CO_2 gas released when the cemented specimen is treated with HCl in closed system under constant volume and temperature (Fukue et al., 2001). Mass of the oven dried (105 °C for 48 h) specimen was measured, and the specimen was placed into the calcimeter flask. HCl (3 mol/L) was placed in small plastic vials and set into the calcimeter flask without spattering the specimen. Subsequently, HCl was allowed to react with specimen in the closed system until the digital manometer (connected with the system) read a constant pressure. From the calibration curve developed between the pressure and $CaCO_3$ content, the carbonate content was estimated, hence the percentage of mass of $CaCO_3$ was determined using the following equation (Eq. (3)).

$$\text{CaCO}_3\ \text{content}(\%) = \frac{\text{Weight of CaCO}_3\ \text{(in the specimen)}}{\text{Weight of the oven dried specimen} - \text{Weight of CaCO}_3} \quad (3)$$

2.5. Freezing and thawing (FT)

Specimens with three different cementation levels were prepared as explained in the previous section. Table 2 presents the detail of the specimens used for freezing-thawing (FT) test. The FT tests were performed in accordance with the methodology suggested in ASTM D 5312-04 (1997). Each FT cycle was subjected to a 12 h of freezing at -20 ± 1 °C followed by a 12 h of thawing at room 25 ± 1 °C. First, specimens were placed in scarp carpeted container, and enough water was added to the container so that the water completely covered the specimens (kept for 12 h). Before subjecting to freezing, enough water was decanted so that the scarp carpet was just immersed. Relatively a fully saturated condition was maintained in the specimens throughout the FT cycles. Experiments were performed in triplicate. The effect of FT cycles on cemented specimens was evaluated by measuring the mass loss, P-wave and S-wave velocities (SonicViewer-SX: 5251, Japan) during the FT test.

2.6. Shear test and equipment

Shear tests were used to investigate the mechanical behavior of heavily cemented MICP treated residual soil. Fig. 3a presents the arrangement of shear test equipment used herein. It is a widely used method to determine the shear strength of soft to hard rocks and cemented specimens by uniaxial compression, firstly suggested by Protodyakonov (1969). The equipment is made of stainless steel, and number of rollers are placed between pressure plate and upper die to eliminate the horizontal displacement of upper die. The cylindrical specimen is placed between two inclined dies attached to the testing machine (Fig. 3b) and sheared along the pre-determined surface. The inclination of the shear plane is determined by the angle (α) of the die is set. There are set of wedges that can adjust the dies and specimen to different angles (Fig. 3b) hence to vary the vertical and tangential components of applied forces and stresses. In this study, for each test condition, three similar specimens were tested at different tilted angles (α of 35°, 40° and 50°). The axis of the cylindrical specimen installed is the same angle as the shearing plane. The machine force (P) is divided into normal force (vertical component to the shear plane) and shear force (along the shear plane) based on the tilted angle of specimen used to shear, and the shear stress (τ) and normal stress (σ) were calculated using Eqs. (4) and (5), respectively. The summary of treated specimens used for the shear test is given in Table 3.

$$\tau = \frac{P}{A}\cos\alpha \quad (4)$$

Table 2
Summary of the specimens used for the FT test.

Level of cementation	No. of cementation injections	Initial V_s (km/sec)	Average $CaCO_3$ content (%)	Specimen No.
Level 1	7	1.00	12.80	7–1
	7	1.05	13.18	7–2
	7	1.06	12.42	7–3
Level 2	10	1.27	17.88	10–1
	10	1.22	16.95	10–2
	10	1.24	17.43	10–3
Level 3	14	1.48	22.76	14–1
	14	1.54	22.01	14–2
	14	1.49	21.86	14–3

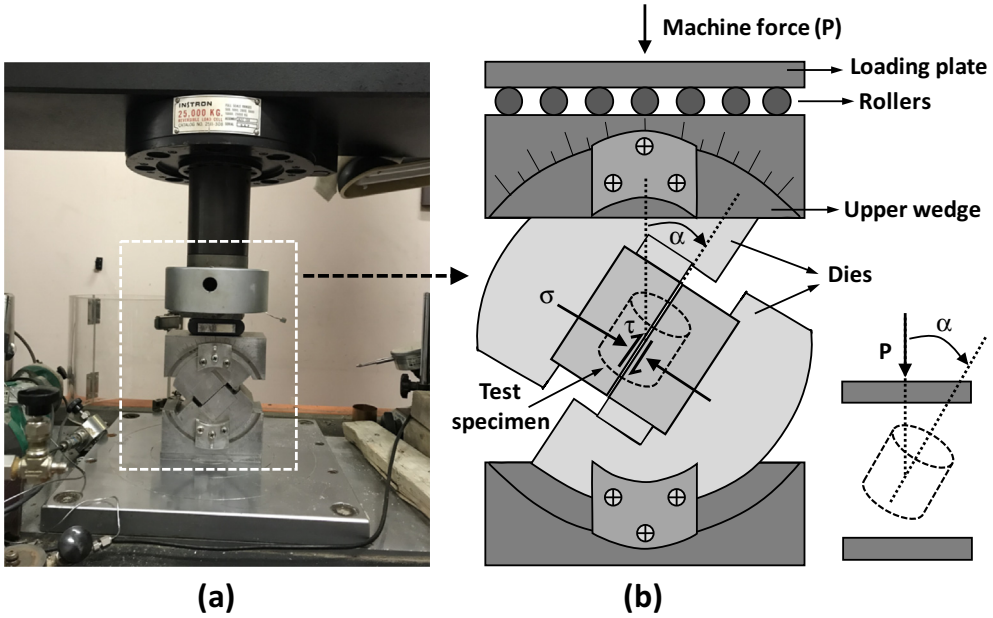

Fig. 3. Shear test equipment setup: (a) the whole system, (b) schematic illustration of the arrangement of shear box, associated system and positioning of test specimen (to the angle α).

Table 3
Summary of the specimens used for the shear test.

Level of cementation	No. of cementation injections	Average $CaCO_3$ content (%)	Inclination angle (α) of specimen tested (°)	Specimen No.
Level 1	7	12.51	35	7–35
	7	12.87	40	7–40
	7	12.76	50	7–50
Level 2	10	16.65	35	10–35
	10	17.11	40	10–40
	10	16.91	50	10–50
Level 3	14	21.27	35	14–35
	14	21.41	40	14–40
	14	22.47	50	14–50

$$\sigma = \frac{P}{A}\sin\alpha \tag{5}$$

As the above Protodyakonov shear test is not applicable for testing loose material, direct shear test was performed to study the shear response of untreated slope soil. The cylindrical specimens (60 mm in diameter; 30 mm in height) were prepared to the similar initial density (1.7 ± 0.1 g/c m^3) of those prepared for MICP treatment, and tests were performed under four different normal pressures (100, 200, 300 and 400 kPa).

2.7. Scanning electron microscopy (SEM)

SEM observations were performed to better understand the effects in the microstructure of MICP specimens.

Specimens were first oven dried at 60 °C, and the representative specimens were collected carefully from the specimen and used for SEM analysis by Miniscope TM 3000, Hitachi (Tokyo, Japan).

3. Results and discussion

3.1. Calcium carbonate and spatial distribution

Cementation level is one of the very important factors that controls the behavior of MICP treated soils. As mentioned earlier, different average carbonate contents were achieved with different number of cementation injections, and the treated specimens are categorized based on the level of cementation (Levels 1, 2 and 3). The measured carbonate content in the untreated residual soil was 0.22–0.25% by mass, and this could be due to the natural presence of calcite, dolomite and siderite. However, the residual carbonate content of slope soil (Onuma, Japan) is relatively negligible compared to that of residual soils reported previously (i.e. 1.35–6.5% by mass) (Lee et al., 2013; Ng et al., 2012). The number of cementation injections (N) and the corresponding precipitated average calcium carbonate content of all the specimens used herein are presented in Tables 2 and 3. It can be seen that the average calcium carbonate content increases gradually with the increase in number of cementation injections. A similar tendency between calcium carbonate content and treatment times was reported by Cui et al. (2017) to the sands cemented to the average calcium carbonate level between 0 and 12%. However, the average mass of calcium carbonate content alone is not appropriate to characterize the MICP treated specimens (Feng and Montoya, 2017), thereby, shear wave velocities were also measured. The shear wave velocities of Level 1, 2 and 3 specimens range 1–1.1 km/s, 1.2–1.3 km/s and 1.45–1.55 km/s, respectively, falling under heavy cementation category as mentioned in previous section. It is worth to note that shear wave velocity below around 0.9 km/s, specimens were unable to withstand their shape under own self-weight.

As MICP is achieved by surface injections, it is highly important to evaluate the spatial distribution of $CaCO_3$. Another set of specimens prepared identically were carefully divided in to three evenly spaced sections along the height (top, middle and bottom), and the calcium carbonate contents were evaluated separately. Fig. 4 presents the spatial variation. The result shows relatively a gradient (i.e. non-uniformity) in the distribution of carbonate content along the height at all the treatment levels. Similar profiles were also reported to the fine grained sands (Cheng and Cord-Ruwisch, 2014; Lin et al., 2016; Zamani et al., 2019). The variation in the precipitation along the depth could be attributed to the distribution of bacteria and pore space distribution (Martinez et al., 2013). During the biological injections, bacteria were filtered by the soil, resulting higher bacteria retainment near injection source compared to the distances away from injection. Also, the

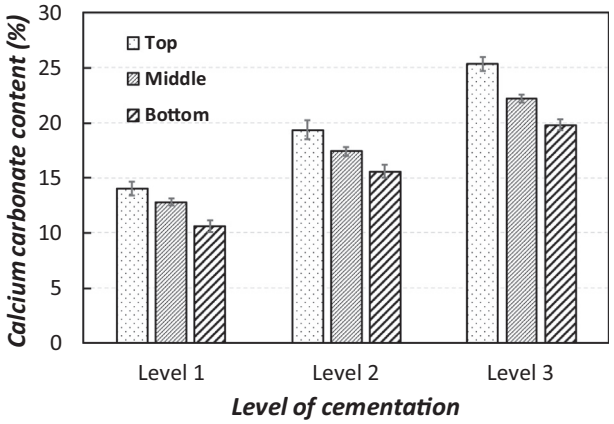

Fig. 4. Calcium carbonate distribution (along the depth) in cemented specimens.

low infiltration rate in fine soils might cause more resource utilization at specimen top, leading less resource supply to bottom soils as suggested by Whiffin et al. (2007). On the other hand, relatively a uniform carbonate precipitation along the specimen was reported to coarse grained sands (Cui et al., 2017; Lin et al., 2016), which is because the bacteria cells and supplied resources can easily flow through the large pore spaces, promoting the uniform cementation along the depth. In this paper, the average carbonate contents were used to represent the cementation levels of the treated specimens.

3.2. Freeze-thaw response

The regions of relatively high latitude (i.e. cold regions) such as Hokkaido, Japan, usually exposed to freeze–thaw (FT) cycles during winter seasons. It is anticipated that similar to soft rocks, FT cycles may induce uneven stresses due to the progressive expansion of the pore water, resulting structural damages and decrease in soil stability. In this research work, slope soil specimens treated to three different cementation levels (Table 2) were subjected to continuous FT cycles; assuming one FT cycle equals to one seasonal frost (one year), the response of MICP specimens were studied for 25 seasonal frosts (i.e. 25 FT cycles).

Hokkaido experiences more than 100 days winter, and soils are covered by considerable layer of snow, keeping the soils continuously to be frozen (temperature ranging from 0 °C to −15 °C) during entire winter (Farukh and Yamada, 2018). Despite of the impairments caused by freezing, the aggregate stability increases at frozen state (Dagesse, 2013; Perfect et al., 1990). When the soils experiences thawing, the aggregate stability drops significantly; as the result, soil losses are typically reported in early spring (on thawed surfaces during snowmelt) (Oztas and Fayetorbay, 2003). On the above basis, therefore, the assumption that the effect of one FT cycle is comparable with one seasonal frost (i.e. long freeze in winter, followed by thawing in early spring), is made. The assumption is

further fortified, as the duration and rate of the freezing were found to have insignificant effect on aggregate stability (Dagesse, 2013; Li and Fan, 2014).

3.2.1. Visual observations and loss in mass

Fig. 5 presents the appearance of the cemented specimens after subjecting repeated FT cycles. The damages in Level 1 cemented specimens could be seen after 5 cycles (Fig. 5a). The signs of damages in Level 2 and Level 3 specimens could be able to see after 15 and 25 cycles, respectively. By the end of 25 cycles, the Level 1 specimens experienced severe damage with separation of cemented pieces (less than 1 cm) and loose soil particles (similar to that of untreated). Relatively a moderate level of damage was observed in Level 2 specimens after 25 cycles (Fig. 5b). Level 3 specimens (Fig. 5c), on the other hand, showed only a minor level of surface damage, indicating higher resistance to continuous FT damages compared to that of Level 1 which is inherently susceptible to severe FT damage.

Fig. 6 compares the cumulative mass loss from the specimens after exposure to FT cycles. The mass loss is severe in Level 1 cemented specimens, which exponentially increases with increasing number of FT cycles. The Level 2 specimens experienced relatively a moderate mass loss: the loss was around 3% after 15 cycles, and thereafter, that increased dramatically to around 20% by the end of 25 cycles, whereas the loss was above 50% in Level 1 cemented specimens. Conversely, at high $CaCO_3$ content (Level 3), loss of mass was negligible (less than 2%), and this response

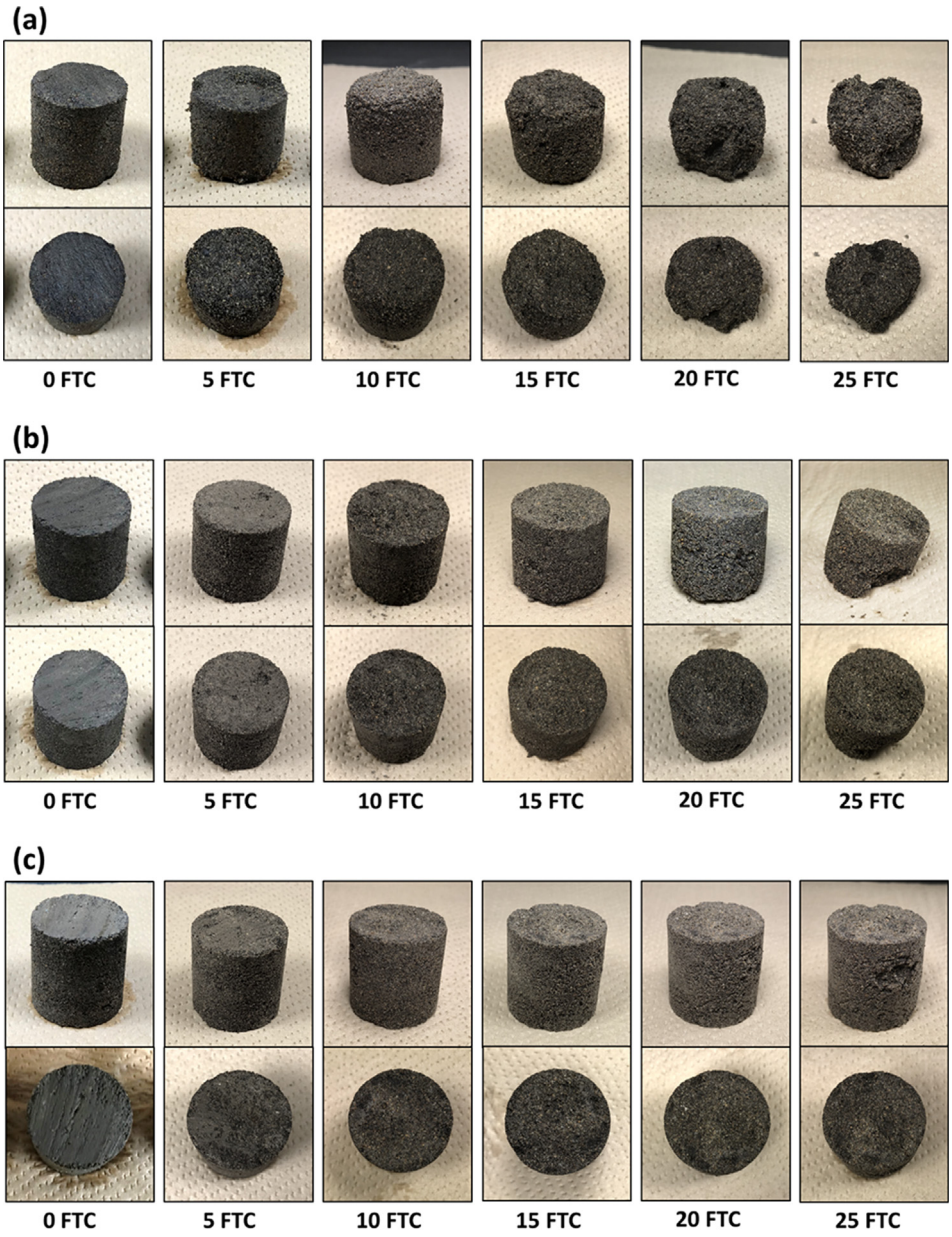

Fig. 5. Appearance of (a) Level 1, (b) Level 2 and (c) Level 3 cemented specimens subjected to repeated FT cycles.

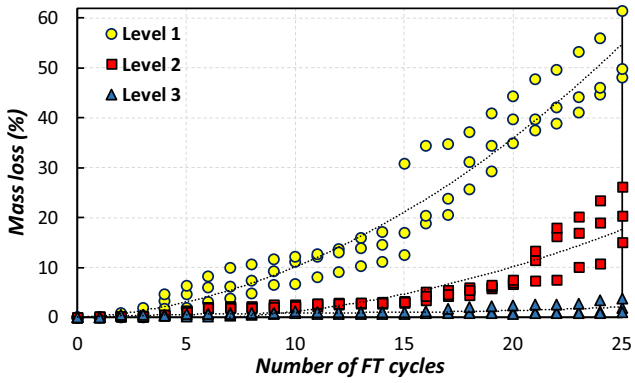

Fig. 6. Mass loss of cemented specimens versus number of FT cycles exposed.

is similar to that observed in ordinary Portland cement and alkali aluminosilicate cement specimens subjected to repeated FT cycles (Matalkah and Soroushian, 2018).

3.2.2. Ultrasonic measurements

Fig. 7 shows the variation of S-wave and P-wave velocities (V_s and V_p) versus number of cycles during FT test. It can be seen that the V_p measurements are slightly higher than the V_s measurements for all the conditions, and that might be attributed to the dominant influence of the porewater on the bulk modulus of saturated specimens. Similar observations were also reported to the saturated sand specimens (Lin et al., 2016). Both S-wave and P-wave velocities show a gradual decrease following FT cycles in both specimens cemented to Level 1 and Level 2. By the end of 15 cycles, S-wave velocities decreased by 20% for Level 1 specimens. As mentioned early, Level 1 specimens exhibited severe damages after 15 cycles (Fig. 5a), and their velocities were unable to be measured precisely. For the Level 2 specimens, they were measurable until 25 FT cycles, and the decrease in V_s was 24% after exposure of complete 25 cycles. On the other hand, the loss in V_s and V_p in Level 3 cemented specimens were only 7.3% and 1.12%. These decrease in both V_s and V_p with increasing FT cycles is

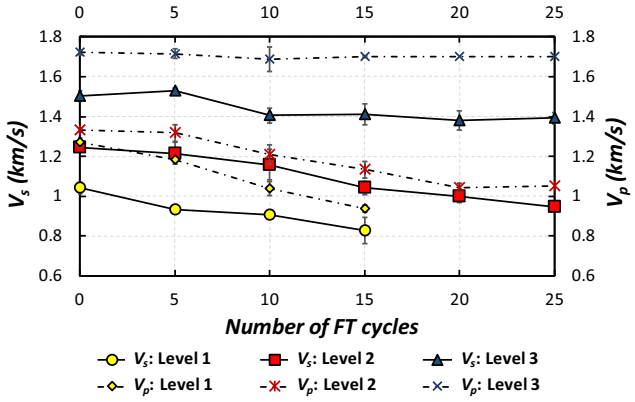

Fig. 7. Variation of S-wave and P-wave velocities (V_s and V_p respectively) of cemented specimens with the continuous FT cycles.

attributed to the formation and evolution of microcracks due to the stresses developed around the soil particles during the freezing of porewater within soil matrix. Although V_s and V_p have shown the decrease, evolution of these microcracks could significantly affect the travel path of S-waves compared to P-waves, resulted high loss in V_s.

These results further reveal that the FT response is highly influenced by the amount of precipitated $CaCO_3$. In fact, the precipitated $CaCO_3$ at particle contacts has the greatest effect on the V_s (Qabany et al., 2011), thereby, more or less of the precipitation content at particle contact would in turn increase or decrease the V_s, respectively (Feng and Montoya, 2017). At the end of the test, Level 3 cemented specimens experienced only a minor decrease in V_s (7.3%) where the loss is high for lower cementation levels (above 20%), suggesting high resistive stresses are attributed to strong contact cementations. Treating the specimens to high cementation (e.g. Level 3) would lead more carbonate precipitation at particle contacts, strengthening the connective bonds (i.e. bridging adjacent particles in voids; strengthening the previously formed bonds). This would contribute to increased resistance for FT effects i.e. formation of ruptures due to the progressive expansion of porewater while turning into ice.

3.2.3. Discussion

Previous studies have demonstrated that seasonal freezing-thawing plays a fundamental role in slope erosion during run-off events that follows thawing (Ferrick and Gatto, 2005; Gatto, 2000; Sadeghi et al., 2018). Typically, the FT cycles largely affects the aggregate stability, which scales-off the residue from the soil matrix, increasing the erodibility potential. MICP treatment enhances the aggregate stability by cementing the particle contacts and sometimes bridging the particles in void spaces, and this bonding facilitates additional resistive forces against the FT effects. The results have demonstrated that level of cementation has a great role in FT response of MICP treated specimens.

By the end of 25 cycles, the SEM analysis was performed to the representative sample carefully taken from Level 1 specimens, and the micrographs are presented in Fig. 8. The observation suggests that the degradation mode occurred during FT cycles is dominantly crystal-soil detachment, compared to the localized cracking of crystals which was barely observed in the soil matrix. Fig. 8 clearly depicts the prints of the soil particles detached from the cementation by the uneven forces developed during the freezing. Fundamentally, the detachment of soil particles from the cementation is controlled by the calcium carbonate precipitation content at the contact points. Higher precipitation content (Level 3) could facilitate the formation of larger and stronger clusters with large contact area at particle contacts, thus reducing the likelihood of crystal-soil detachment. In the case of Level 1, the particle bonds were comparatively weak, and that could easily be ruptured or detached during FT cycles. It should also be

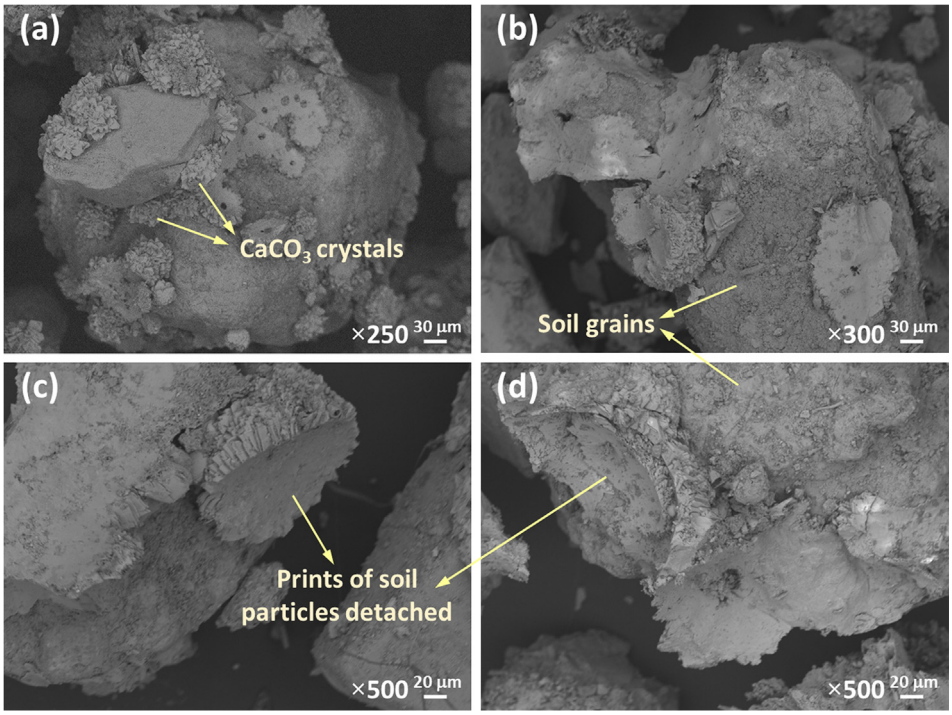

Fig. 8. Footprints of crystal-soil detachment, the degradation mode of FT effects captured in SEM of the representative sample of Level 1 specimen.

noted, despite of considerable damages witnessed in MICP matrix, there were no observable microstructural damages identified in individual soil particles by the end of the cycles.

There are many factors that control the FT response of soil matrix, including particle size distribution, water content, soil texture, number of cycles and freezing temperature (Behzadfar et al., 2017; Cheng et al., 2016; Oztas and Fayetorbay, 2003). Among them, particle size distribution has a major role in determining freezing-thawing behavior of MICP treated specimens, as the MICP behaviors significantly vary with different grain sizes (Dhami et al., 2016; Oliveira et al., 2016). Previously, many studies have confirmed that soils dominated by large aggregates could withstand more against cyclic FT, as their high porosity led to the rapid water flows and movements (Oztas and Fayetorbay, 2003; Viklander, 2011). However, recently, Cheng et al. (2016) have demonstrated that the FT response of MICP cemented sands differ from typical response of untreated sands, in which the number of contacts per soil particles governs the behavior. The number of particle contacts per soil sphere increases with the decrease in porosity, and thereby, contact points per particle increases when the average grain size decreases from coarse to fine. Comparing the behavior of MICP treated fine sand (D_{50}, 0.15 mm) with coarse sand (D_{50}, 1.18 mm), the coarse sand exposed to FT cycles shown significant drop in unconfined compressive strength (UCS) compared to that of fine sand (Cheng et al., 2016). Larger particle contacts in fine sand could decrease the resultant tensile stress (aroused from freezing) acted per particle and exhibited more durability. For the well-graded sand, further enhancement in FT resistance was reported due to the presence of both coarse and fines contributing high permeability and high particle contacts, respectively. The slope soil investigated in this study is fine grained soil (D_{50}, 0.23 mm), consisting particles ranging from very fine to medium sands (Fig. 2a). It has been reported that compared to the uniformly graded sands, the well-graded soils often have a greater number of particle contacts (Gowthaman et al., 2019b), which also seems comparable to the slope soil studied herein. Furthermore, moisture content is one of the important factors, which could govern the stress levels to be applied in treated soils during freezing process.

This study has verified that MICP technique with the required level of cementation can be used to stabilize the slope soil against freezing-thawing that affect the aggregate stability and erodibility of soil deposits. The adequate treatment could cement the particle contacts sufficiently, enhancing the resistance to the formation of ruptures and crystal-soil detachments due to uneven tensile stresses developed during the frost of porewater. The design life of the treatment can also be approximately determined based on the results presented (i.e. relating number of seasonal frosts with number of FT cycles). For example, it can be roughly said that soils treated to the average $CaCO_3$ content of 12–14%, 16–18% and 21–23% by mass can effectively withstand against freeze–thaw erosions for 5, 15 and 25 years of service. One of the issues that is often reported in the current existing slope stabilization techniques is significant loss in permeability of treated soils, interrupt the

flow lines of ground water, leads to increase in porewater pressure, perhaps resulting failures and structural collapse. The MICP treatment by surface percolation technique (Cheng et al., 2013; Cheng and Cord-Ruwisch, 2014) could provide numerous advantages, particularly in field implementation stages, that allows MICP solutions to retain at particle contacts, leading effective formation of crystals at contact points. That could also retain higher permeability in treated soil matrix compared to the existing methods such as soil cementation by Portland cement. It is worth noting that the permeability retention leads no excess water build-up on treated surface during runoff and snow-melt, thereby, eliminating the additional facilitation of drainage systems.

3.3. Shear response of cemented soil

A set of drained shear tests were performed on cemented slope soils treated to different cementation levels (Table 3). As explained in previous section, specimens were sheared at different inclined angles, and the responses of the MICP specimens cemented to Level 1, 2 and 3 are illustrated in Fig. 9a, b and c, respectively, where the shear and corresponding normal stresses are provided against shear strain. It can be seen that the distribution of shear and normal stresses are dependent on the angle held during the shearing. The normal stress changes together with the shear stress (based on α), and peak of the specimen would occur when the shear-normal stress point reaches the failure envelope. It can also be observed (Fig. 9) that there is a significant difference in stress curves at 40° and 50° inclination conditions. In fact, at α of 50°, the normal stresses (Eq. (5)) are higher than the corresponding shear stresses (Eq. (4)). Increasing machine force coupled with the high component of normal stress lead the specimens to undergo over compression during the shearing at 50°. This over compression effect was often encountered during the shearing with the inclination of above 50° (Protodyakonov, 1969; Vutukuri et al., 1974); under the high compression, the shear resistance increased substantially, resulting the failure of specimens at high magnitudes.

Based on the stress–strain results (Fig. 9), the failure envelopes of MICP cemented specimens corresponding to both peak state and residual state conditions were obtained simply as suggested by Protodyakonov (1969). The failure envelopes were derived by plotting the shear stresses against the normal stresses of the specimens sheared at different inclined angles, and then by connecting all the peak or residual state points of tests. The obtained peak and residual strength envelopes of all three cementation levels are compared with that of untreated in Fig. 10 and Fig. 11, respectively. It can be seen that relatively linear failure envelopes are obtained for all the cementation levels. Similar linear envelopes were also reported to the sands treated to light to moderate cementation levels (Cui et al., 2017; Feng and Montoya, 2016).

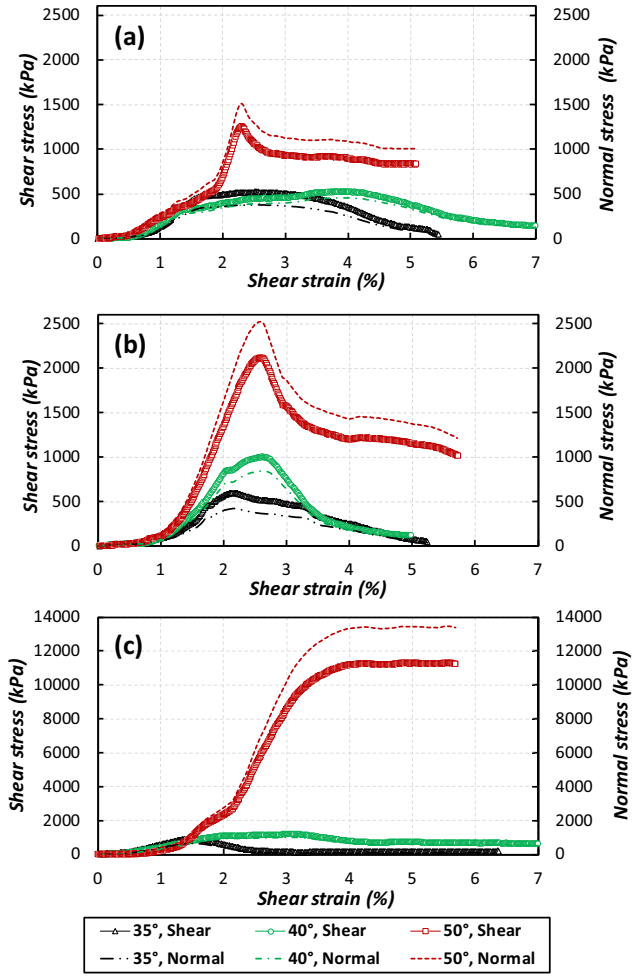

Fig. 9. Stress–strain relationships of the slope soils cemented to (a) Level 1, (b) Level 2 and (c) Level 3 at different angles held during the test.

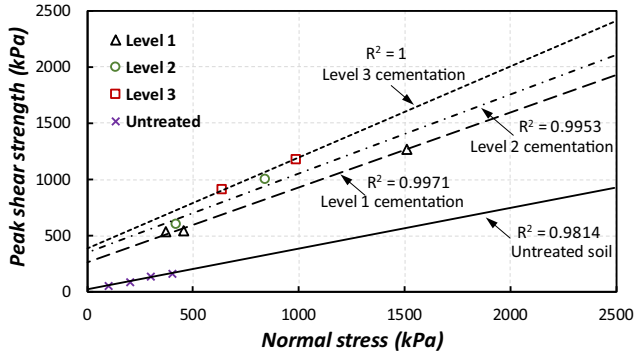

Fig. 10. Peak shear strength envelopes of cemented slope soil specimens (the envelopes of Level 1, 2 and 3 specimens were from Protodyakonov shear test, and the envelope of untreated one was from direct shear test).

3.3.1. Peak and residual shear strength

Fig. 10 presents the peak shear strengths (τ_{peak}) of the cemented specimens at different heavy cementation levels. As expected, the τ_{peak} values of the cemented specimens increase with the increase in normal stress (i.e. vertical con-

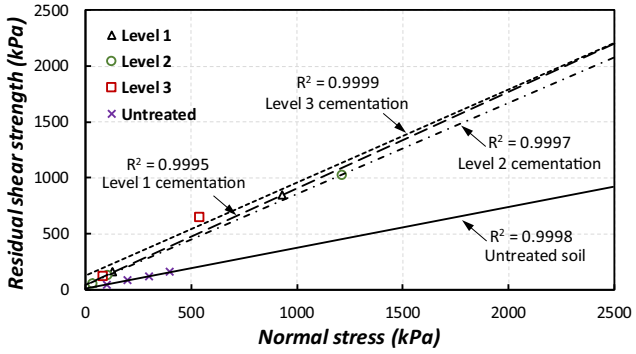

Fig. 11. Residual shear strength envelopes of cemented slope soil specimens (the envelopes of Level 1, 2 and 3 specimens were from Protodyakonov shear test, and the envelope of untreated one was from direct shear test).

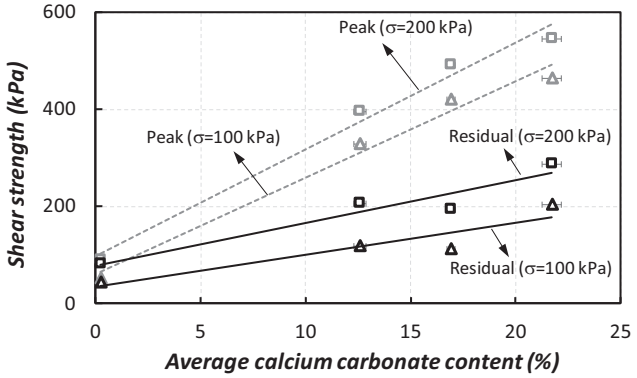

Fig. 12. Variation of shear strength with the precipitated carbonate content (under 100 kPa and 200 kPa normal confining pressures).

fining pressure), regardless of cementation level. It also can be seen that the specimens exhibit high τ_{peak} values compared to that of untreated soil of similar initial relative density. A comparison of untreated and bi-cemented specimen indicates that the τ_{peak} value increased by an average of 520% for the Level 1 cementation, 695% for the Level 2 and 780% for the Level 3 cementation compared with the τ_{peak} value of untreated specimen at a normal pressure of 100 kPa. It is worth noting, the failure envelopes clearly reveal that the peak shear strength is attributed to both friction and cohesion components at these levels of MICP cementation.

The residual shear strengths (τ_{res}) of the cemented specimens against normal confining stress are shown in Fig. 11. MICP treatment has increased τ_{res} values of residual slope soil, similar to that observed for τ_{peak}. However, under similar normal stress, the increase in τ_{res} with the increase in cementation levels is not high as observed in behavior of τ_{peak} (Fig. 10). The results further demonstrate that the residual state envelope is also a straight line with relatively low cohesion which is very close to that of untreated soil, suggesting minimal portion of strength increase attributed to cohesion. This is consistent with the previous observation by Montoya and De Jong (2015).

For the stability analysis of slope surfaces, the strength parameters at low stress ranges are highly necessary (Panta, 2018). As the MICP treats the near-surface zone of the slopes, it is important to understand the state of the strength with respect to the level of cementation to ensure the safety and serviceability. Therefore, the τ_{peak} and τ_{res} are plotted against cementation levels under 100 and 200 kPa normal stresses and presented in Fig. 12. The shear strengths of different cementation levels were estimated from the failure envelopes (Fig. 10 and Fig. 11). The results show that the τ_{peak} and τ_{res} linearly increase with the increase in cementation level, and this increase of τ_{peak} is similar to that of bio-cemented residual soils reported by Lee et al. (2013). Under 100 kPa normal stress, the τ_{res} of specimens increased by average factors of 2.7 and 4.7 respectively for Level 1 and Level 3 cementation, whereas the τ_{peak} increased by average factors of 6.2 and 8.8 relative to those of untreated specimens.

During the shearing, the specimens showed a loss of strength after the peak stress, until residual state is reached. The cemented specimens showed relatively a sharp loss of in stress upon reaching the peak point, but this summit was not observed in shear stress–strain response of untreated specimen (results are not presented in this paper). This post-peak strength loss in untreated soil is around 9.5 kPa at 100 kPa normal confining pressure. At the same normal stress, the losses are around 210, 251 and 315 kPa for the specimens cemented to Level 1, 2 and 3 respectively. It is clear that the loss of post-peak strength increases with the increase in cementation level, suggesting the increase in brittleness. Similar brittle type failures are also experienced by Lee et al. (2013) and Montoya et al. (2013).

3.3.2. Shear strength parameters

To further understand the improvement in shear strength of cemented specimens, effective friction angle (ϕ') and cohesion (c') were calculated from the shear test results based on the Mohr-Coulomb failure criterion. The variations of friction angles and cohesions with average carbonate contents are presented in Figs. 13 and 14, respectively. The peak (ϕ'_p) and residual friction (ϕ'_r) angles for the untreated soils are 21° and 20°, respectively, and the associated cohesions are 16 and 7 kPa (c'_p and c'_r, respectively). The internal friction angles obtained herein are likely to be lower than the typical friction angle values reported to sandy soils (Cui et al., 2017; Montoya and De Jong, 2015). For instance, a uniform sand with similar mean particle diameter has been reported to have the friction angle of around 24° (Cheng et al., 2013). Basically, the friction angle of the soil is governed by several factors such as grain size, grain shape, surface roughness, mineralogy, fines, organic content and moisture level (Bareither et al., 2008; Canakci et al., 2016). Herein, the discrepancy could possibly be due to the presence of fines and organic contents. The residual slope soil studied herein consists of around 12% of fines (i.e. <125 μm), and which could

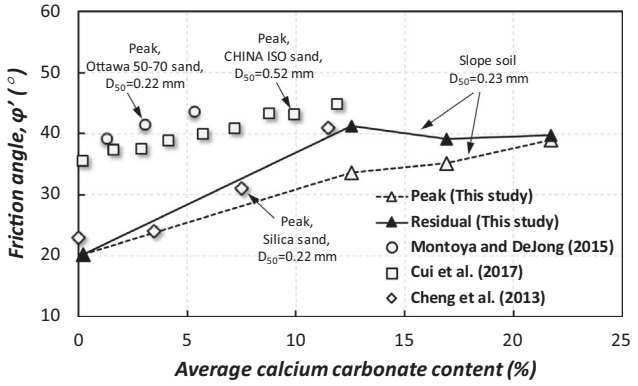

Fig. 13. Variation of peak and residual friction angle with the average calcium carbonate content.

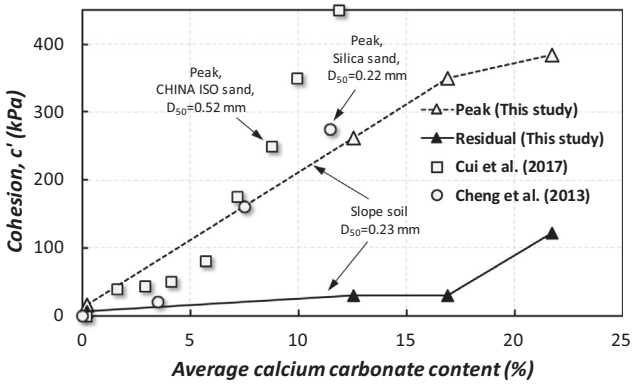

Fig. 14. Variation of peak and residual cohesion with the average calcium carbonate content.

contribute to the easy slip between the aggregates in the shear environment. Few previous studies also witnessed the considerable decrease by 3 − 5° in friction angle when the fine content increase to around 10% (Phan et al., 2016). In addition, in this study, the soils were used at its natural state, i.e. no pretreatments were undertaken to eliminate the impurities from the soil. In fact, an observable quantity of organic material (such as decomposed plant substances, organic fines, etc.) was widely witnessed in the soil, and the presence of organic fines on shearing planes also could adversely result on friction angle.

Fig. 13 clearly illustrates that the increase in cementation results in an increase in ϕ'_p of all tested levels. The peak friction angles range around 33.5°, 35° and 39° for Level 1, 2 and 3 cemented specimens, respectively, depicting relatively a linear increase. The tendency of ϕ'_p versus carbonate content are in a very good agreement with the results reported by many researchers (Cheng et al., 2013; Cui et al., 2017; Montoya and De Jong, 2015) (Fig. 13). Cementation has also resulted a remarkable increase in c'_p (Fig. 12), and similar observations were also reported by Cheng et al. (2013) and Cui et al. (2017).

It is also found that the trend of ϕ'_r is similar to that of ϕ'_p; however, the cemented soils demonstrate larger ϕ'_r than the ϕ'_p at all levels of cementation. On the other hand, the cohesion parameters at residual state is significantly lower than that at peak state (Fig. 14). For example, c'_p of Level 1 cemented soil was 261 kPa, and that dropped drastically by an average factor of 8.5 at residual state, resulting small amount c'_r. Lin et al. (2016) have reported that the c'_r of MICP cemented sand was similar to the c'_r of untreated sand. A similar residual cohesion also was reported to the sands treated by Portland cement (Clough et al., 1981). These results suggest that the residual shear strength of slope soil is predominantly frictional with a minimum portion of the strength attributed by cohesion at these cementation levels.

3.3.3. Discussion

Based on the results presented herein, bio-cementation appears to have influence on both friction angle and cohesion strength parameters for soils at heavy cementation levels. Previously, Feng and Montoya (2016) have demonstrated that the effect of MICP on the cohesion strength parameter is limited in lightly and moderately cemented sands. Following the investigation, this study has demonstrated that the above conclusion is not applicable for soils cemented heavily (above 12% $CaCO_3$). During the MICP treatment process, the $CaCO_3$ crystals coat the soil particles and cement them at contact points (DeJong et al., 2010). At low cementation levels (0–3.5%), precipitated carbonate crystals are insufficient to provide effective bonding at particle contacts, and the crystals could randomly precipitate within the soil matrix while increasing the dry density, leading to increase only the friction angle parameters significantly (Cheng et al., 2013; Feng and Montoya, 2016). On the other hand, higher calcium carbonate content could develop strong interparticle connections, thereby enhancing both the friction angle and cohesion parameters (Figs. 13 and 14).

Once the maximum shear resistance is reached, localized shearing occurs with the breakage of inter particle connections (initiate with the yielding of crystals), eventually resulting the loss of effective cementation and associated peak strength. However, the specimens exhibited higher residual strength compared to that of untreated slope soil at the cementation levels investigated herein (12–23%), which is primarily due to the frictional parameter. Fig. 15 confirms that high cementations increase the particle roughness significantly by coating the soils. The representative specimens taken from the middle of the sheared plane (after the shearing test) were observed through SEM. The specimens cemented to Level 1, 2 and 3 are illustrated in Fig. 15a, 15b and 15c, respectively. The observation suggests that the high cementation leads more crystal formation on particle surface in addition to the contact cementations. During the residual shearing, these crystals localized on the surface have provided shear resistance by interlockings, and that would possibly be the reason for the increase in residual friction angle. Friction at residual state is also contributed by degraded calcium carbonate crystals produced from the shearing process (Montoya

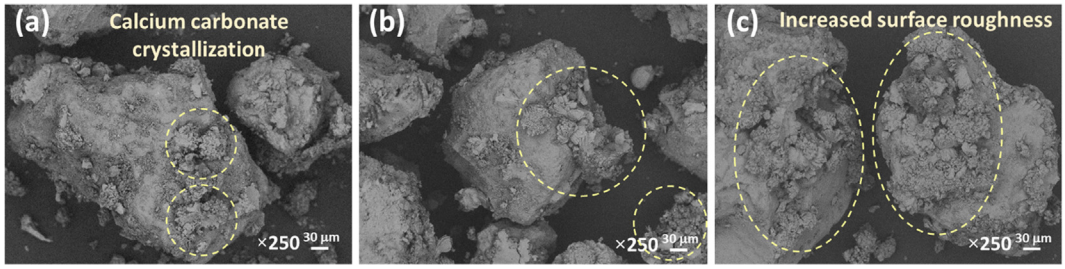

Fig. 15. SEM images of representative samples collected from the sheared plane of (a) Level 1, (b) Level 2 and (c) Level 3 cemented specimens.

and De Jong, 2015). Overall, it can be concluded that the cementation at particle contact attributes to the peak shear strength, whereas the precipitation occurred on particle surfaces attributes to the residual strength.

Previous studies have demonstrated that the increase in cementation level leads to a transition in stress–strain behavior of specimens to strain softening from strain hardening (Feng and Montoya, 2016; Montoya et al., 2013; Mujah et al., 2017). Moreover, Montoya and De Jong (2015) have performed the undrained triaxial loading on sand and reported that the increase in cementation level increases the peak shear stress ratio, but those peak shear stress ratios are obtained at low axial strains.

4. Field implementation and challenges

Fig. 16 depicts the conceptual diagram of the MICP implication to slope soil stabilization. As illustrated in the diagram, the idea is to promote the cover condition of the expressway slope using the novel MICP technique, and thereby to achieve high aggregate stability and to control the excess infiltration. In fact, slopes are more vulnerable to the climatic changes (i.e. winters, rainfall). Seasonal freezing-thawing could result the detachment of aggregates; snowmelt and rainwater runoff as drivers promotes the erosion, resulting movement of aggregates near surface followed by their transportation to downslope (Zhang et al., 2018). At the same time, excess infiltration of water into slope may contribute to the potential for increasing pore water pressure, resulting drop in effective stress of the slope soil. It may further affect the influence of matric suction of soil by lessening the negative pore pressure, resulting the loss in strength in slope soil (Gowthaman et al., 2019b; Harden and Scruggs, 2003). This research work targets to introduce the MICP technique in promoting the cover condition of the slope which attributes to the stability of the slopes.

During the implementation, MICP treatment can be performed by surface percolation i.e. introducing the chemicals simply through the slope surface. The bacteria culture and chemicals can move deeper into the soil pores, that meantime allows the cementation at particle contacts, enhancing the aggregate stability and strength. However, one of the widely observed limitation in MICP technique is achieving homogeneous cementation (Cheng et al., 2013; Martinez et al., 2013). The precipitated calcium carbonate could bond the particles together, densify the soil by reducing the void ratio (Montoya and DeJong 2015),

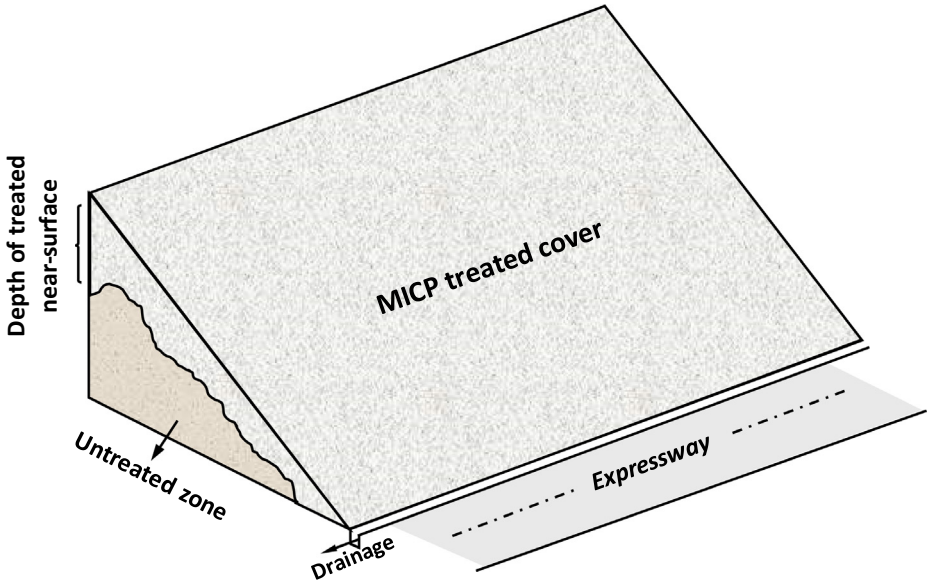

Fig. 16. Conceptual diagram of MICP implemented stabilized expressway slope.

leading to bio-clogging, often reported to fine grained soils (Cheng and Cord-Ruwisch, 2014). As the slope soil investigated herein falls under the category of fine sand, retention of in-situ permeability is an important concern, that would also provide advantage to the engineers during reconstruction phases with additional treatments, so that the design strength and stability could be controlled. Therefore, more investigations should focus on permeability and infiltration rates during treatment process and optimizing the methods to enhance the treatment homogeneity.

As shown in Fig. 1, scaling-up is to be performed in a subsequent phase of this work prior to the field application, and that is highly essential to develop the field treatment methodology and to evaluate the limitations posed by the boundary effects. As discussed by Gowthaman et al. (2019b), the spraying method would be the most feasible and economic approach in large-scale and field applications rather than simple injections, and that has to be investigated in detail. Production of bacteria culture in large-scale (m^3 capacity) is also likely to be another challenge during field application. Considering the cost-effectiveness and transportation challenges, researchers have proposed and demonstrated the use of *in-situ* custom-built reactors as one of the most effective solutions (Omoregie et al., 2020; Whiffin, 2004). Very recently, the possible use of the stirred tank reactor has been demonstrated at the field to desirably produce 3 m^3 of *Sporosarcina pasteurii* by Omoregie et al. (2020). However, to fully overcome this key hurdle, more possible developments and subsequent applications are necessary. The MICP, on the other hand, is not completely environment-friendly, that sources harmful ammonium ions to the ground during the process (van Paassen et al., 2010). The lasting solution containing ammonium ions requires to be removed before contaminating ground water, and associated field monitoring methods also should be developed during field implementation.

5. Conclusions

This paper presented a series of experiments performed to investigate the freeze–thaw durability and shear responses of MICP treated soil, representative of erosion prone expressway slope (Hokkaido, Japan). In fact, the current study is an initiative to understand the effect of freezing-thawing of MICP cemented soils on erosion, and to deepen the understanding of mechanical responses. With the following drawn conclusions, the results have demonstrated the feasibility of newly emerged MICP technique as a viable alternative for slope soil stabilization.

The results from free-thaw tests have revealed that the MICP treated slope soils are durable to the freeze–thaw induced erosion, and however, the level of cementation highly determines the aggregate stability. The specimens cemented to an average of 11–13% ($CaCO_3$ by mass) results high erodibility (50% mass loss), whereas the 20–23% cemented specimens show only a minor erosion (2% mass loss), when they are subjected to 25 cyclic frosts. The similar tendency is also observed in ultrasonic measurements. The high durability of MICP treated soils is primarily attributed to adequate cementation level which facilitates effective particle contacts that could resist the evolution of ruptures hence crystal-soil detachments when the uneven tensile stresses develop around the cemented soil particles during frosting process of pore water.

The results obtained from the shear tests have shown the mechanical behavior of MICP treated slope soil is similar to that of sands. Finding also confirmed that cementation at particle contact attributes to the peak strength, increasing both friction angle and cohesion strength parameters. However, particle roughness i.e. crystals precipitated on soil surface attributes to the residual strength. Cementation level has a great influence in shear response, increasing the peak and residual strengths with the increase in average carbonate content. High post peak loss is observed for the specimens with high cementation level, suggesting increase in brittleness.

Acknowledgement

Authors would like to express the gratitude to Hokkaido Office, East Nippon Expressway Company Limited, Sapporo, Hokkaido, Japan for providing the research opportunity to Hokkaido University, Sapporo, Hokkaido, Japan.

Declaration of Competing Interest

The authors declare no conflict of interest.

References

Amarakoon, G.G.N.N., Kawasaki, S., 2018. Factors affecting sand solidification using MICP with *Pararhodobacter* sp. Mater. Trans. 59, 72–81. https://doi.org/10.2320/matertrans.M-M2017849.

ASTM D5312-92, 1997. Standard Test Method for Evaluation of Durability of Rock for Erosion Control Under Freezing and Thawing Conditions, ASTM International. West Conshohocken, PA. https://doi.org/10.1520/D5312-92R97.

Bao, R., Li, J., Li, L., Cutright, T.J., Chen, L., 2017. Effect of Microbial-Induced Calcite Precipitation on Surface Erosion and Scour of Granular Soils Proof of Concept. J. Transp. Res. Board 2657, 10–18. https://doi.org/http://dx.doi.org/10.3141/2657-02.

Bareither, C.A., Edil, T.B., Benson, C.H., Mickelson, D.M., 2008. Geological and physical factors affecting the friction angle of compacted sands. J. Geotech. Geoenvironmental Eng. 134, 1476–1489. https://doi.org/10.1061/(ASCE)1090-0241(2008)134:10(1476).

Behzadfar, M., Sadeghi, S.H., Khanjani, M.J., Hazbavi, Z., 2017. Effects of rates and time of zeolite application on controlling runoff generation and soil loss from a soil subjected to a freeze-thaw cycle. Int. Soil Water Conserv. Res. 5, 95–101. https://doi.org/10.1016/j.iswcr.2017.04.002.

Canakci, H., Hamed, M., Celik, F., Sidik, W., Eviz, F., 2016. Friction characteristics of organic soil with construction materials. Soils Found. 56, 965–972. https://doi.org/10.1016/j.sandf.2016.11.002.

Cheng, L., Cord-Ruwisch, R., 2014. Upscaling effects of soil improvement by microbially induced calcite precipitation by surface percolation. Geomicrobiol. J. 31, 396–406. https://doi.org/10.1080/01490451.2013.836579.

Cheng, L., Cord-Ruwisch, R., Shahin, M.A., 2013. Cementation of sand soil by microbially induced calcite precipitation at various degrees of saturation. Can. Geotech. J. 50, 81–90. https://doi.org/10.1139/cgj-2012-0023.

Cheng, L., Shahin, M.A., Mujah, D., 2016. Influence of key environmental conditions on microbially induced cementation for soil stabilization. J. Geotech. Geoenvironmental Eng. 143, 04016083. https://doi.org/10.1061/(asce)gt.1943-5606.0001586.

Clough, W., Rad, N.S., Bachus, R.C., Sitar, N., 1981. Cemented sands under static loading. J. Geotech. Eng. Div. 107, 799–817.

Cui, M.J., Zheng, J.J., Zhang, R.J., Lai, H.J., Zhang, J., 2017. Influence of cementation level on the strength behaviour of bio-cemented sand. Acta Geotech. 12, 971–986. https://doi.org/10.1007/s11440-017-0574-9.

Dagesse, D.F., 2013. Freezing cycle effects on water stability of soil aggregates. Can. J. Soil Sci. 93, 473–483. https://doi.org/10.4141/CJSS2012-046.

Danjo, T., Kawasaki, S., 2016. Microbially induced sand cementation method using *Pararhodobacter* sp. strain SO1, inspired by beachrock formation mechanism. Mater. Trans. 57, 428–437. https://doi.org/10.2320/matertrans.M-M2015842.

DeJong, J.T., Fritzges, M.B., Nüsslein, K., 2006. Microbially induced cementation to control sand response to undrained shear. J. Geotech. Geoenvironmental Eng. 132, 1381–1392. https://doi.org/10.1061/(asce)1090-0241(2006)132:11(1381).

DeJong, J.T., Mortensen, B.M., Martinez, B.C., Nelson, D.C., 2010. Bio-mediated soil improvement. Ecol. Eng. 36, 197–210. https://doi.org/10.1016/j.ecoleng.2008.12.029.

Dhami, N.K., Reddy, M.S., Mukherjee, A., 2016. Significant indicators for biomineralisation in sand of varying grain sizes. Constr. Build. Mater. 104, 198–207. https://doi.org/10.1016/j.conbuildmat.2015.12.023.

Farukh, M.A., Yamada, T.J., 2018. Synoptic climatology of winter daily temperature extremes in Sapporo, northern Japan. Int. J. Climatol. 38, 2230–2238. https://doi.org/10.1002/joc.5329.

Feng, K., Montoya, B.M., 2017. Quantifying level of microbial-induced cementation for cyclically loaded sand. J. Geotech. Geoenvironmental Eng. 143, 06017005. https://doi.org/10.1061/(ASCE)GT.1943-5606.0001682.

Feng, K., Montoya, B.M., 2016. Influence of confinement and cementation level on the behavior of microbial-induced calcite precipitated sands under monotonic drained loading. J. Geotech. Geoenvironmental Eng. 142, 04015057. https://doi.org/10.1061/(ASCE)GT.1943-5606.0001379.

Ferrick, M.G., Gatto, L.W., 2005. Quantifying the effect of a freeze-thaw cycle on soil erosion: laboratory experiments. Earth Surf. Process. Landforms 30, 1305–1326. https://doi.org/10.1002/esp.1209.

Fox, D.M., Bryan, R.B., Price, A.G., 1997. The influence of slope angle on final infiltration rate for interrill, conditions. Geoderma 80, 181–194. https://doi.org/10.1016/S0016-7061(97)00075-X.

Fukue, M., Nakamura, T., Kato, Y., 2001. A method for determining carbonate content for soils and evaluation of the results. Soils Found. (in Japanese) 49–2, 9–12.

Gatto, L.W., 2000. Soil freeze-thaw-induced changes to a simulated rill: Potential impacts on soil erosion. Geomorphology 32, 147–160. https://doi.org/10.1016/S0169-555X(99)00092-6.

Gowthaman, S., Iki, T., Nakashima, K., Ebina, K., Kawasaki, S., 2019a. Feasibility study for slope soil stabilization by microbial induced carbonate precipitation (MICP) using indigenous bacteria isolated from cold subarctic region. SN Appl. Sci. 1, 1480. https://doi.org/10.1007/s42452-019-1508-y.

Gowthaman, S., Mitsuyama, S., Nakashima, K., Komatsu, M., Kawasaki, S., 2019b. Biogeotechnical approach for slope soil stabilization using locally isolated bacteria and inexpensive low-grade chemicals: a feasibility study on Hokkaido expressway soil, Japan. Soils Found. 59, 484–499. https://doi.org/10.1016/j.sandf.2018.12.010.

Harden, C.P., Scruggs, P.D., 2003. Infiltration on mountain slopes: a comparison of three environments. Geomorphology 55, 5–24. https://doi.org/10.1016/S0169-555X(03)00129-6.

Jiang, N.-J., Soga, K., 2019. Erosional behavior of gravel-sand mixtures stabilized by microbially induced calcite precipitation (MICP). Soils Found. 59, 699–709. https://doi.org/10.1016/j.sandf.2019.02.003.

Jiang, N.-J., Tang, C.-S., Yin, L.-Y., Xie, Y.-H., Shi, B., 2019. Applicability of microbial calcification method for sandy-slope surface erosion control. J. Mater. Civ. Eng. 31, 04019250. https://doi.org/10.1061/(ASCE)MT.1943-5533.0002897.

Jiang, N.J., Soga, K., 2017. The applicability of microbially induced calcite precipitation (MICP) for internal erosion control in gravel–sand mixtures. Géotechnique 67, 42–55. https://doi.org/10.1680/jgeot.15.P.182.

Kværnø, S.H., Øygarden, L., 2006. The influence of freeze-thaw cycles and soil moisture on aggregate stability of three soils in Norway. Catena 67, 175–182. https://doi.org/10.1016/j.catena.2006.03.011.

Lee, M.L., Ng, W.S., Tanaka, Y., 2013. Stress-deformation and compressibility responses of bio-mediated residual soils. Ecol. Eng. 60, 142–149. https://doi.org/10.1016/j.ecoleng.2013.07.034.

Li, G.Y., Fan, H.M., 2014. Effect of freeze-thaw on water stability of aggregates in a black soil of Northeast China. Pedosphere 24, 285–290. https://doi.org/10.1016/S1002-0160(14)60015-1.

Lin, H., Suleiman, M.T., Brown, D.G., Kavazanjian, E., 2016. Mechanical Behavior of Sands Treated by Microbially Induced Carbonate Precipitation. J. Geotech. Geoenvironmental Eng. 142, 04015066-1–13. https://doi.org/10.1061/(ASCE)GT.1943-5606.0001383.

Martinez, B.C., DeJong, J.T., Ginn, T.R., Montoya, B.M., Barkouki, T. H., Hunt, C., Tanyu, B., Major, D., 2013. Experimental optimization of microbial-induced carbonate precipitation for soil improvement. J. Geotech. Geoenvironmental Eng. 139, 587–598. https://doi.org/10.1061/(ASCE)GT.1943-5606.0000787.

Matalkah, F., Soroushian, P., 2018. Freeze thaw and deicer salt scaling resistance of concrete prepared with alkali aluminosilicate cement. Constr. Build. Mater. 163, 200–213. https://doi.org/10.1016/j.conbuildmat.2017.12.119.

Meyer, F.D., Bang, S., Min, S., Stetler, L.D., Bang, S.S., 2011. Microbiologically-Induced Soil Stabilization: Application of Sporosarcina pasteurii for Fugitive Dust Control, in: Geo-Frontiers 2011. American Society of Civil Engineers, Reston, VA, pp. 4002–4011. https://doi.org/10.1061/41165(397)409.

Montoya, B.M., De Jong, J.T., 2015. Stress-strain behavior of sands cemented by microbially induced calcite precipitation. J. Geotech. Geoenvironmental Eng. 141. https://doi.org/10.1061/(ASCE)GT.1943-5606.0001302.

Montoya, B.M., DeJong, J.T., Boulanger, R.W., 2013. Dynamic response of liquefiable sand improved by microbial-induced calcite precipitation. Géotechnique 63, 302–312. https://doi.org/10.1680/geot.sip13.p.019.

Mujah, D., Shahin, M.A., Cheng, L., 2017. State-of-the-art review of biocementation by microbially induced calcite precipitation (MICP) for soil stabilization. Geomicrobiol. J. 34, 524–537. https://doi.org/10.1080/01490451.2016.1225866.

Ng, W., Lee, M., Hii, S., 2012. An overview of the factors affecting microbial-induced calcite precipitation and its potential application in soil improvement. World Acad. Sci. Eng. Technol. 6, 188–194.

Oliveira, P.J.V., Freitas, L.D., Carmona, J.P.S.F., 2016. Effect of soil type on the enzymatic calcium carbonate precipitation process used for soil improvement. J. Mater. Civ. Eng. 29, 1–7. https://doi.org/10.1061/(ASCE)MT.1943-5533.0001804.

Omoregie, A.I., Palombo, E.A., Ong, D.E.L., Nissom, P.M., 2020. A feasible scale-up production of *Sporosarcina pasteurii* using custom-built stirred tank reactor for in-situ soil biocementation. Biocatal. Agric. Biotechnol. 24. https://doi.org/10.1016/j.bcab.2020.101544 101544.

Oztas, T., Fayetorbay, F., 2003. Effect of freezing and thawing processes on soil aggregate stability. Catena 52, 1–8. https://doi.org/10.1016/S0341-8162(02)00177-7.

Panta, A., 2018. Strength characteristics of fine-grained soils at dyke slope surfaces. Doctoral thesis, Hokkaido University, Japan. https://doi.org/10.14943/doctoral.k13346.

Perfect, E., Van Loon, W.K.P., Kay, B.D., Groenevelt, P.H., 1990. Influence of ice segregation and solutes on soil structural stability. Can. J. Soil Sci. 70, 571–581. https://doi.org/10.4141/cjss90-060.

Phan, V.T.A., Hsiao, D.H., Nguyen, P.T.L., 2016. Effects of fines contents on engineering properties of sand-fines mixtures. Procedia Eng. 142, 213–220. https://doi.org/10.1016/j.proeng.2016.02.034.

Protodyakonov, M.M., 1969. Methods of determining the shearing strength of rocks, in: Mechanical Properties of Rocks. Israel Program for Scientific Translations, pp. 15–27.

Qabany, A. Al, Mortensen, B., Martinez, B., Soga, K., Dejong, J., 2011. Microbial carbonate precipitation: Correlation of S-wave velocity with calcite precipitation. Geotechnical Special Publication. American Society of Civil Engineers, Reston, VA, pp. 3993–4001. https://doi.org/10.1061/41165(397)408.

Rieke-Zapp, D.H., Nearing, M.A., 2005. Slope Shape Effects on Erosion. Soil Sci. Soc. Am. J. 69, 1463. https://doi.org/10.2136/sssaj2005.0015.

Sadeghi, S.H., Raeisi, M.B., Hazbavi, Z., 2018. Influence of freeze-only and freezing-thawing cycles on splash erosion. Int. Soil Water Conserv. Res. 6, 275–279. https://doi.org/10.1016/j.iswcr.2018.07.004.

Salifu, E., MacLachlan, E., Iyer, K.R., Knapp, C.W., Tarantino, A., 2016. Application of microbially induced calcite precipitation in erosion mitigation and stabilisation of sandy soil foreshore slopes: a preliminary investigation. Eng. Geol. 201, 96–105. https://doi.org/10.1016/j.enggeo.2015.12.027.

Soon, N.W., Lee, L.M., Khun, T.C., Ling, H.S., 2014. Factors affecting improvement in engineering properties of residual soil through microbial-induced calcite precipitation. J. Geotech. Geoenvironmental Eng. 140, 04014006. https://doi.org/10.1061/(ASCE)GT.1943-5606.0001089.

van Paassen, L.A., Ghose, R., van der Linden, T.J.M., van der Star, W.R. L., van Loosdrecht, M.C.M., 2010. Quantifying biomediated ground improvement by ureolysis: large-scale biogrout experiment. J. Geotech. Geoenvironmental Eng. 136, 1721–1728. https://doi.org/10.1061/(ASCE)GT.1943-5606.0000382.

Viklander, P., 2011. Permeability and volume changes in till due to cyclic freeze/thaw. Can. Geotech. J. 35, 471–477. https://doi.org/10.1139/t98-015.

Vutukuri, V.S., Lama, R.D., Saluja, S.S., 1974. Handbook on Mechanical Properties of Rocks: Testing Techniques and Results, Vol. 1. ed. Trans Tech Publications, Clausthal, Germany.

Wang, Y., Soga, K., Dejong, J.T., Kabla, A.J., 2019. Microscale visualization of microbial-induced calcium carbonate precipitation processes. J. Geotech. Geoenviron. Eng. 145, 1–13. https://doi.org/10.1061/(ASCE)GT.1943-5606.0002079.

Whiffin, V.S., 2004. Microbial $CaCO_3$ Precipitation for the Production of Biocement. West. Aust. Murdoch Univ. Perth. https://doi.org/http://researchrepository.murdoch.edu.au/399/2/02Whole.pdf.

Whiffin, V.S., van Paassen, L.A., Harkes, M.P., 2007. Microbial carbonate precipitation as a soil improvement technique. Geomicrobiol. J. 24, 417–423. https://doi.org/10.1080/01490450701436505.

Zamani, A., Montoya, B., Gabr, M., 2019. Investigating the challenges of in situ delivery of MICP in fine grain sands and silty sands. Can. Geotech. J. https://doi.org/10.1139/cgj-2018-0551.

Zhang, X., Hu, M., Guo, X., Yang, H., Zhang, Z., Zhang, K., 2018. Effects of topographic factors on runoff and soil loss in Southwest China. Catena 160, 394–402. https://doi.org/10.1016/j.catena.2017.10.013.